NKS-446
ISBN 978-87-7893-538-0

WPS-MAF, Report on design and results from experimental test program for material characterization

Tobias Bolinder[1]
Alexander Eriksson[1]
Jonas Faleskog[2]
Magnus Boåsen[2]
Sebastian Lindqvist[3]
Veera Peltonen[3]

[1]Kiwa Inspecta Technology AB, Stockholm, Sweden

[2]Royal Institute of Technology, Department of Solid Mechanics
Stockholm, Sweden

[3]VTT, Helsinki, Finland

April 2021

Abstract

In this report, the VTT and KTH experimental results are presented. The characterization of the ductile to brittle transition region was done with small 5x10 single-edge bend specimens (SE(B)) and 15x30 SE(B) specimens in different temperatures. The characterization with 15x30 SE(B) specimens were done with deep and shallow cracks. The characterization was completed by metallography characterization of the 533B plate. This is an interim report related to the characterization and development work done in WPS-MAF. The results are utilized later in the project.

Key words

Warm pre-stressing, Cleavage fracture, Failure probability, Fracture toughness, Fracture experiments, Non-local probabilistic model, Master Curve

NKS-446
ISBN 978-87-7893-538-0
Electronic report, April 2021
NKS Secretariat
P.O. Box 49
DK - 4000 Roskilde, Denmark
Phone +45 4677 4041
www.nks.org
e-mail nks@nks.org

WPS-MAF, Report on design and results from experimental test program for material characterization

Report from the NKS-R WPS-MAF (Contract: AFT/NKS-R(20)132/8)

Tobias Bolinder[1], Alexander Eriksson[1]
Jonas Faleskog[2], Magnus Boåsen[2]
Sebastian Lindqvist[3], Veera Peltonen[3]

[1]Kiwa Inspecta Technology AB, Stockholm, Sweden
[2]Royal Institute of Technology, Department of Solid Mechanics, Stockholm, Sweden
[3]VTT, Helsinki, Finland

Table of content ***Page***

1 INTRODUCTION

Brittle fracture is a disastrous event that can occur in components of ferritic steels at lower temperatures. In this temperature range the steel experience a significantly lower fracture toughness and the fracture is typically associated with sudden structural collapse. This region is called the lower shelf region of the material fracture toughness curve. The problem is usually avoided entirely by ensuring that the component is operated in a temperature range where the steel is ductile enough, i.e. the upper shelf region. This is, however, not always possible. One such example is when considering operation beyond 40 years of the reactor pressure vessel (RPV) in a nuclear power plant, long term operation (LTO). Irradiation induced embrittlement of the RPV shifts the temperature range for the ductile region of the steel in such a way that certain loading conditions can lead to difficulties in demonstrating safe operation when using traditional assessment methods. These are typical cases where the warm pre-stressing effect (WPS effect) is beneficial, such that an analysis accounting for this phenomenon will show enough margin to fracture to ensure safe operation.

This research project aims to answer what the margin and probability of fracture is during the cooling part of a typical pressurized thermal shock (PTS) transient in a RPV. For this to be possible a non-local probabilistic model for cleavage fracture that accounts for effects of load history and changes in temperature will be developed. To be able to develop such a model a large experimental program has been conducted during 2020.

In this report, the VTT and KTH experimental results are presented. The characterization of the ductile to brittle transition region was done with small 5x10 single-edge bend specimens (SE(B)) and 15x30 SE(B) specimens in different temperatures. The characterization with 15x30 SE(B) specimens were done with deep and shallow cracks. The characterization was completed by metallography characterization of the 533B plate. This is an interim report related to the characterization and development work done in WPS-MAF. The results are utilized later in the project and are planned to be presented in journal articles.

2 GOAL

The goal with the experimental program described within this report is to characterize the fracture toughness in the ductile-to-brittle transition region in different temperatures and with various crack lengths. This is a prerequisite for the planned development of the WPS model.

3 MATERIAL

3.1 TEST MATERIAL

Figure 1 shows the A533 grade B class 1 plate from a top view. The yellow arrow at the center indicates the rolling direction. The plate was 400 mm wide, 500 mm long, and 230 mm thick. The 5x10 SE(B) specimens were cut from the 100 mm wide slice also used in another project. Two sides of the plate were flame cut and two sides were cut with a band saw.

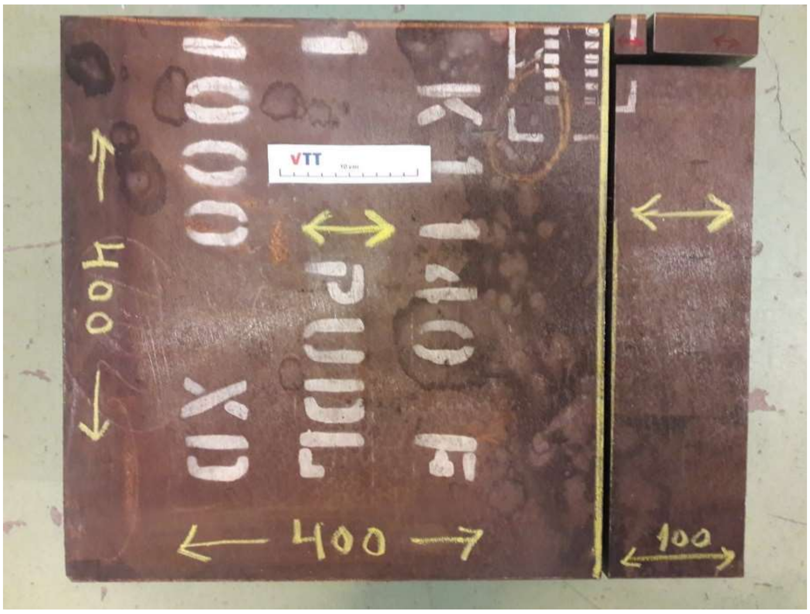

Figure 1. Test material, A533B type plate.

The material in this study originates from IAEA research activities. Similar material has been used as a 'reference steel' in surveillance programmes for a reliable comparison irradiation embrittlement behavior. The material was designated as 'JRQ', introduced by the IAEA in the Co-ordinated Research Project on "Optimizing Reactor Pressure Vessel Surveillance Programmes and their Analysis", which began in 1983. The JRQ plate was manufactured in Japan by the Kawasaki Steel Corporation. The plate in this study has the designation JRQ, it originates from Japan [1].

The JRQ steel was produced by the BOF-LRF (basic oxygen furnace process and ladle refining furnace). After rolling, the plates were heat treated:

- normalizing at 900 °C
- quenching from 880 °C
- tempering at 665 °C for 12 hours,
- stress relieving at 620 °C for 40 hours.

3.2 TEST SPECIMENS AND MATRIX

The testing was done with single edge bend (SE(B)) specimens, figure 2. Both 5 mm thick (B) and 10 mm wide (W) 5x10 SE(B) specimens and 15 mm thick and 30 mm wide SE(B) specimens were applied to investigate the effect of the specimen size. For the 15x30 SE(B) specimens two crack lengths (a) were used, a/W = 0.1 and a/W = 0.5 to investigate the effect of shallow cracks on fracture toughness these data are also needed in the development of the numerical model in WP 2. The crack length for the 5x10 SE(B) was a/W = 0.5.

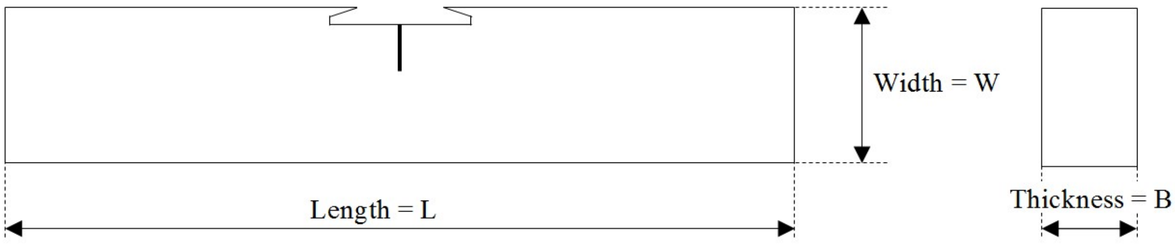

Figure 2. Schematic image of the SE(B) specimen.

Table 1 shows the test matrix. The orientation of the specimens was L-T, the crack grows transverse to the rolling direction and the normal of the fracture surface is in the longitudinal direction.

Table 1. Test matrix.

Specimen	Orientation	Test temperature [°C]	Crack length a/W	Number of specimens
5x10 SE(B)	L-T	-115 (avg)	0.5	12
15x30 SE(B)	L-T	-70	0.5	8
15x30 SE(B)	L-T	-85	0.5	8
15x30 SE(B)	L-T	-100	0.5	7
15x30 SE(B)	L-T	-120	0.5	9
15x30 SE(B)	L-T	-160	0.5	8
15x30 SE(B)	L-T	-70	0.1	8
15x30 SE(B)	L-T	-85	0.1	8
15x30 SE(B)	L-T	-100	0.1	8
15x30 SE(B)	L-T	-120	0.1	8
15x30 SE(B)	L-T	-160	0.1	8

3.3 CUTTING OF THE SPECIMENS

The specimens were cut from the plate with an electro-discharge wire cutter (EDWC). Figure 3 shows the location from where the 5x10 SE(B) specimens were cut. Figures 4 and 5 show the cutting plan for the 15x30 SE(B) specimens.

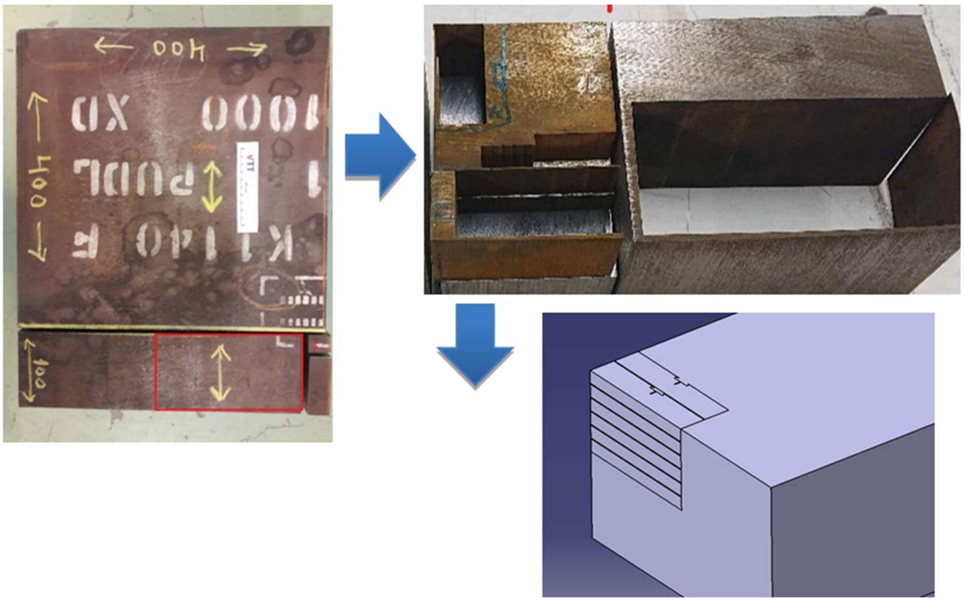

Figure 3. Cutting of the 5x10 SE(B) specimens. In average, the specimens were located 65 mm from the surface.

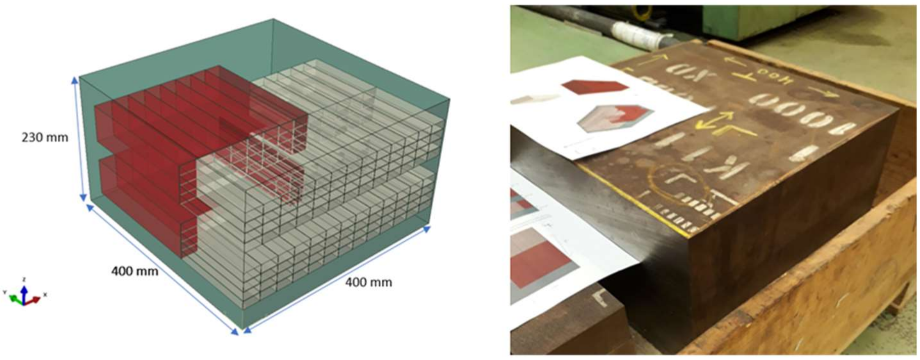

Figure 4. Cutting plan, for the testing programme planned for 2020-2021.

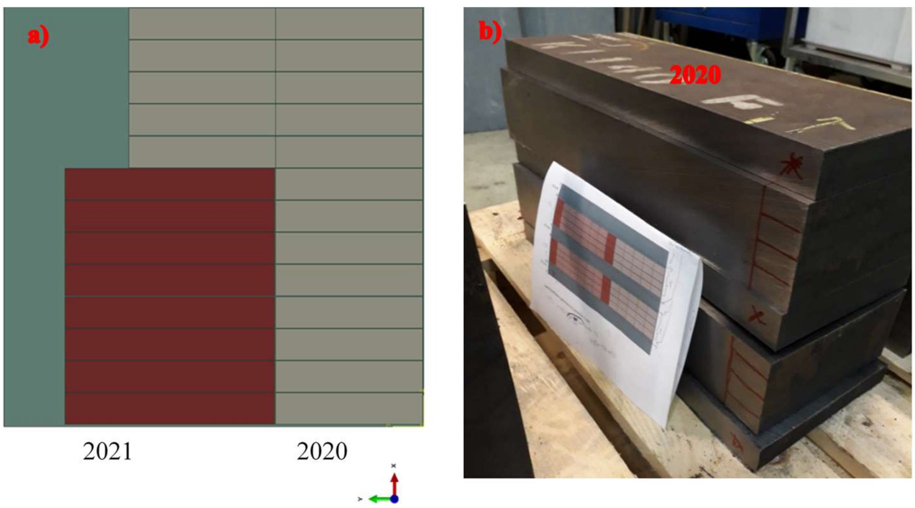

Figure 5. a) top view of the plate. The grey squares are the 15x30 SE(B) specimens. b) First cut. The surface parts and the central parts of the plate were not used. The goal was to ensure that the specimens were cut from a location with as homogeneous properties as possible. The specimens in the column with the red squares will be tested in 2021.

Figure 6 shows how the specimens were named. The specimens selected for each series were randomly sampled. Each series has a distinctive colour. Table 3shows how the specimens were divided between the different series.

Figure 6. Side-view of the plate. The 15x30 SE(B) specimens cut in 2020. The specimens from the same series have the same colour. Random sampling was used to ensure that the different series would have equal amount of specimens from the different layers.

Table 2. Tabell of each individual specimens for each test serie.

Series	Specimen ID
15x30 SE(B), a/W = 0.5, T = -120	Y1.6, Y2.2, Y2.12, Y3.8, Y4.4, Y4.13, A1.2, A2.6
15x30 SE(B), a/W = 0.5, T = -100	Y1.8, Y3.4, Y2.13, Y3.10, Y4.2, Y4.6, A1.4, A3.2
15x30 SE(B), a/W = 0.5, T = -160	Y1.2, Y1.13, Y2.6, Y2.10, Y3.13, Y4.12, A3.4, A4.6
15x30 SE(B), a/W = 0.5, T = -85	Y1.10, Y1.4, Y2.8, Y3.12, Y4.10, A1.6, A2.2, A4.4
15x30 SE(B), a/W = 0.5, T = -70	Y1.12,Y2.4, Y3.2, Y3.6, Y4.8, A2.4, A3.6, A4.2
15x30 SE(B), a/W = 0.1, T = -100	Y1.1, Y2.7, Y3.3, Y3.9, Y4.5, A2.5, A3.7, A4.1
15x30 SE(B), a/W = 0.1, T = -120	Y1.5, Y3.1, Y4.9, Y4.11, A1.3, A3.1, A3.5, A4.7
15x30 SE(B), a/W = 0.1, T = -160	Y1.3, Y1.9, Y2.1, Y2.11, Y3.5, Y4.7, A1.1, A2.3
15x30 SE(B), a/W = 0.1, T = -85	Y1.11, Y2.5, Y3.7, Y4.3, A1.5, A2.1, A2.7, A4.3
15x30 SE(B), a/W = 0.1, T = -70	A1.7, A3.3, A4.5, Y1.7, Y2.3, Y2.9, Y3.11, Y4.1

4 METHODS

4.1 METALLOGRAPHY, HARDNESS AND OES

The elementary analysis was performed with optical emission spectrometry (OES). The locations for the analyses are 2, 5.5, and 9.5 cm from the surface, figure 7, shown together with the locations for the microsections. OES analysis 1 and microsections 1.1 and 1.2 were done from the sample extracted close to the surface of the plate. The metallography was done from the surface aligned along the rolling direction and from a surface perpendicular to the rolling direction. The hardness measurements were performed with the Vickers tip (HV10). The hardness was measured through the thickness. The indentation spacing was 10 mm. The hardness through the thickness was measured three times, from three adjacent lines.

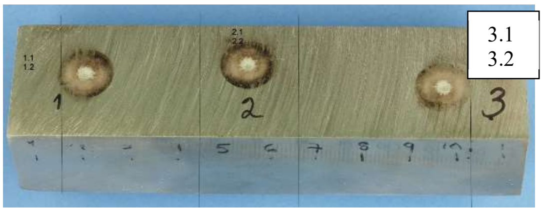

Figure 7. Locations of OES analyses and microsections.

4.2 FRACTURE TOUGHNESS

The fracture mechanical characterisation was done by following ASTM E1921 standard as closely as possible. Below the different labs VTT and KTH describes the procedures used in the testing:

VTT

The pre-cracking of the specimens by VTT was done with Rumul Testronic resonant testing machine in three-point bending fatigue, with the R-value being 0.1. The goal of the a_0/W-values were 0.1 and 0.5, depending on the series. The specimens were tested at VTT using the MTS 250 kN load frame. MTS Basic TestWare application was used to control and run the tests. The testing temperatures were achieved with a conventional environmental chamber and liquid nitrogen. The crack mouth opening was measured with MTS clip gauge and the temperature was measured from the surface of the specimen with K-type thermocouples taped to the specimen.

KTH

The pre-cracking of the specimens at KTH Solid Mechanics was carried out using a servo-hydraulic testing machine in three-point bending fatigue, with the R-value being 0.1. The specimens were pre-cracked to a_0/W -ratios of 0.1 and 0.5, where the 0.1-series were monitored using strain gauges to achieve the correct crack lengths and the 0.5-series were monitored using a clip-gauge. The specimens were tested at KTH Solid Mechanics inside a cooling chamber, cooled using liquid nitrogen and a thermocouple mounted close to the crack tip of the specimen. Loading was applied using a constant rate of displacement in a servo-hydraulic testing machine with a load capacity of 100 kN using the controller MTS FlexTest 60 and the in-house control program TensileUn in the MTS TestSuite application to run and control the testing. Force, piston displacement and crack mouth opening displacement (CMOD) was continuously recorded during the testing.

5 RESULTS

5.1 HARDNESS AND CHEMESTRY

The hardness of the material was measured through the whole thickness; the hardness profile is presented in figure 8 and measurement locations in figure 9. The plate is hardest at the surface and softest at the center.

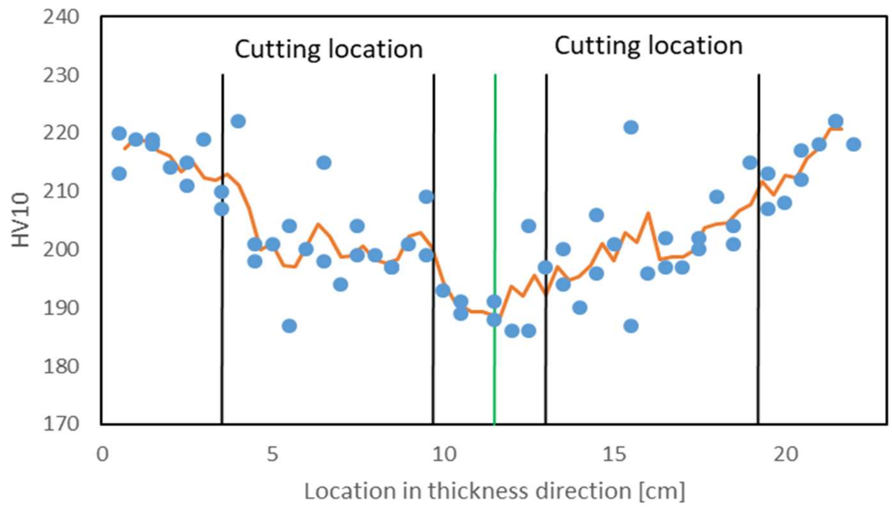

Figure 8. Hardness profile in thickness direction of 533B plate.

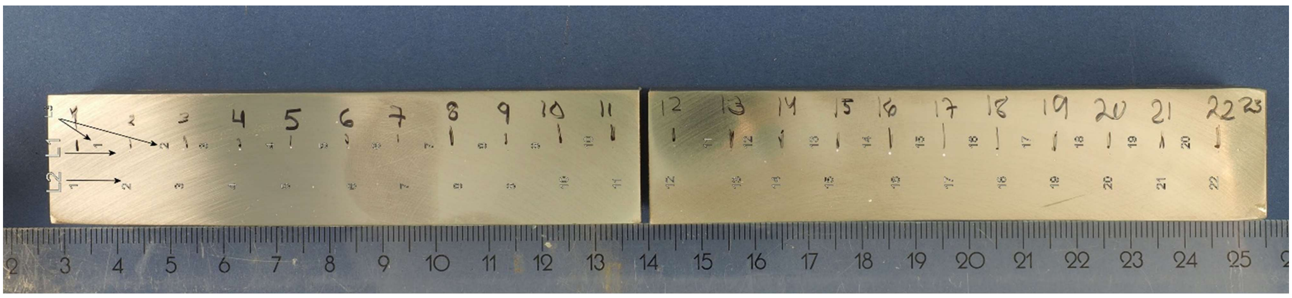

Figure 9. Locations of hardness measurements.

Hardness HV10 correlates to the yield strength, σ_{ys}, equations 1 and 2.

$$HV = \sigma_{flow} \cdot 3.5/9.8 \tag{1}$$

$$\sigma_{flow} = \sigma_{ys}\left\{1 + \left(\frac{C_2}{\sigma_{ys}}\right)^2\right\} \tag{2}$$

Figure 10 shows the flow stress levels. It is assumed that the hardness behaves symmetrically relative to the center of the plate, and thus, the results are presented relative to the center.

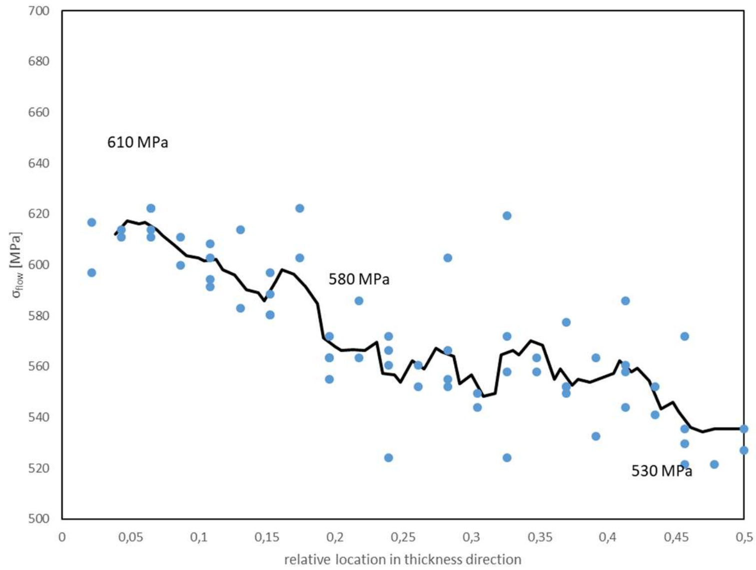

Figure 10. Variation in flow stress behaviour in the thickness direction of the plate, estimated based on hardness HV10.

Table 3 shows that there are no significant differences in chemical content in the different depth locations, 2 cm (surface), 5.5 cm, and 9.5 (center) cm from the surface.

Table 3. Chemical content in the depth direction of the plate.

Specimen	Composition [%]															
	C	Si	Mn	S	P	Cr	Ni	Mo	Cu	Al	W	V	Ti	Co	Nb	B
OES1	0.17	0.24	1.43	0.006	0.017	0.13	0.84	0.50	0.15	0.017	<0.01	0.005	0.002	0.006	0.003	<0.0005
OES2	0.18	0.24	1.42	0.007	0.017	0.13	0.85	0.49	0.16	0.017	<0.01	0.005	0.002	0.006	0.003	<0.0005
OES3	0.18	0.24	1.42	0.006	0.016	0.13	0.83	0.50	0.15	0.018	<0.01	0.006	0.002	0.006	0.003	<0.0005

5.2 METALLOGRAPHY

Figures 11 and 14 show the change in the macrostructure when moving from the surface towards the center of the plate. Close to the surface there are no segregation lines, but farther from the surface the segregation lines start to appear, and the lines seem to be more frequent closer to the center. The texture of the microstructure varies in the different orientations, figure 15.

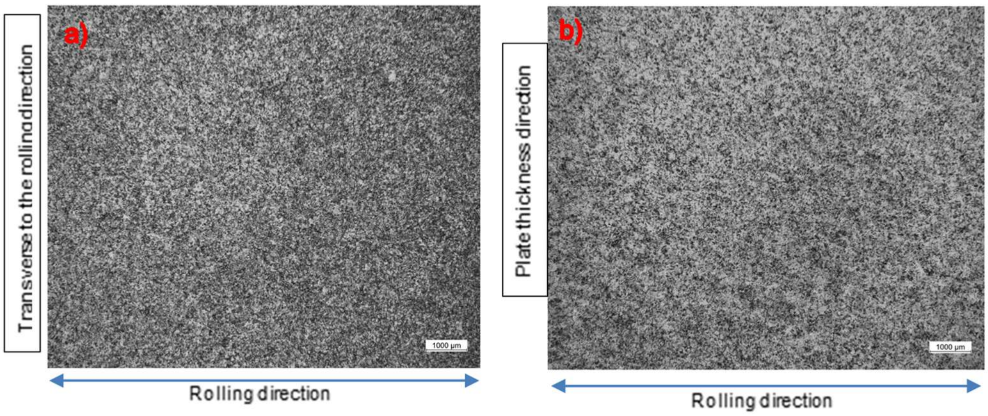

Figure 11. The sample is extracted 2 cm from the surface, 11x9 mm^2. a) In the rolling direction, b) opposite to the rolling direction.

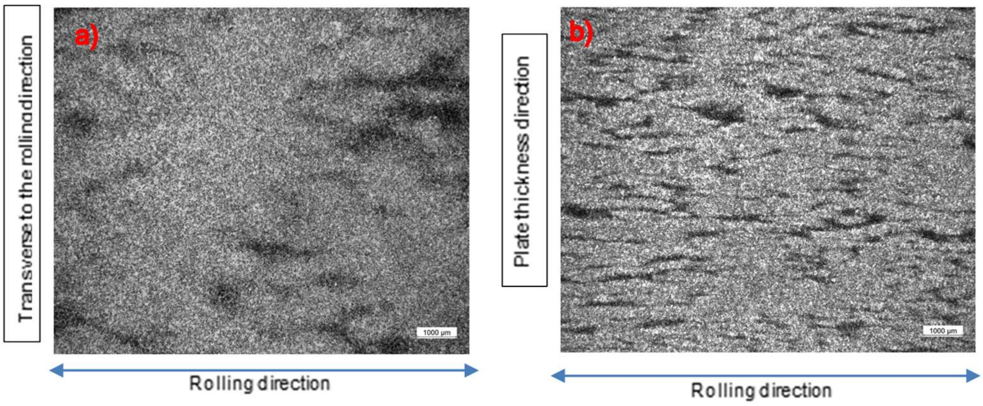

Figure 12. The sample is extracted 5.5 cm from the surface, 11x9 mm^2. a) In the rolling direction, b) opposite to the rolling direction.

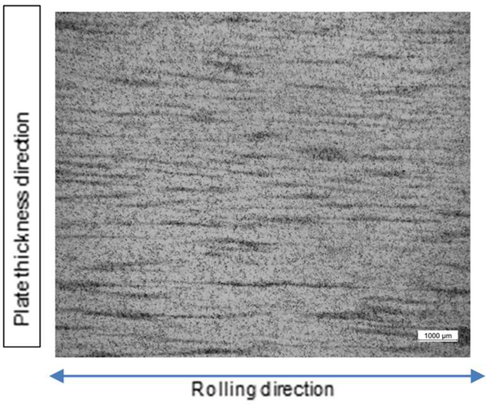

Figure 13. The sample is extracted 9.5 cm from the surface, 11x9 mm^2.

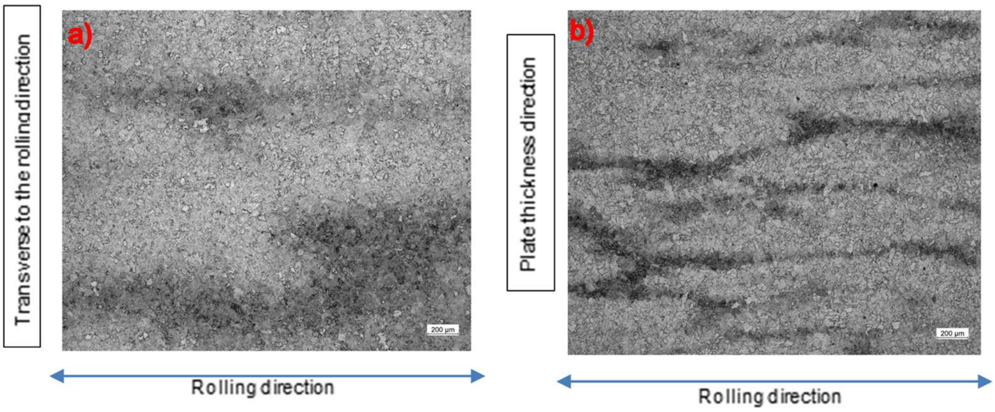

Figure 14. The sample is extracted 9.5 cm from the surface, ≈ 2.5x2.5 mm^2. a) In the rolling direction b) opposite to the rolling direction.

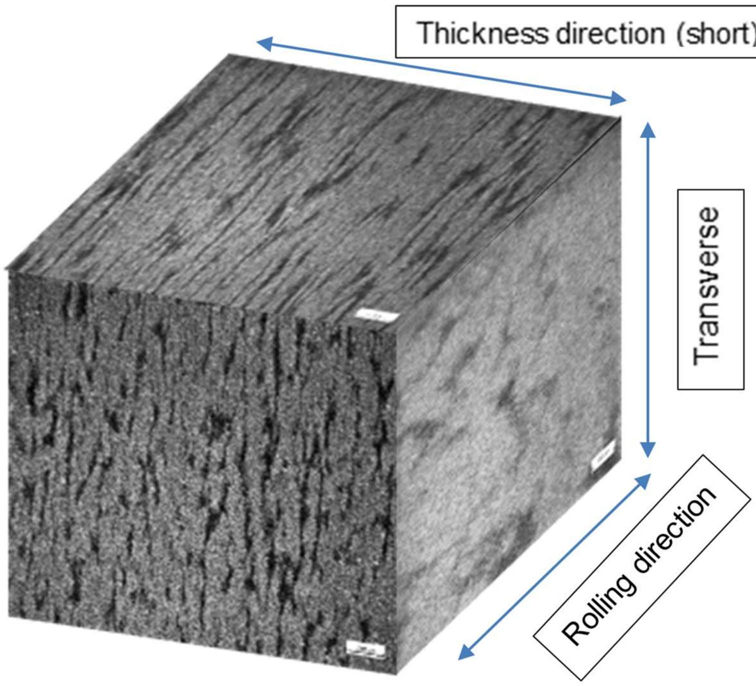

Figure 15. The microstructure in the different orientations.

5.3 FRACTURE TOUGHNESS

The fracture toughness results are presented in Table 4 to Table 13. Young's Moduli are determined as $E = 204 - \frac{T}{16}$, where E is the Young's Modulus and T is the average testing temperature.

Table 4. Results of the test series 15x30 SE(B), a/W = 0.5, T = -160 °C.

Specimen	W [mm]	B [mm]	Bn [mm]	a0 [mm]	b0 [mm]	E [GPa]	KJc [MPa]	KJc(1T) [MPa]	T [°C]
A3.4	30,00	14,99	11,95	15,40	14,60	214	31	30	-161
A4.6	30,00	14,96	11,95	15,48	14,52	214	29	28	-161
Y1.2	29,98	15,00	12,01	15,42	14,56	214	37	35	-161
Y1.13	29,88	14,87	11,97	15,50	14,38	214	57	52	-161
Y2.6	29,97	14,96	12,00	15,37	14,60	214	43	40	-161
Y2.10	29,98	14,97	11,85	15,55	14,43	214	52	48	-161
Y3.13	29,92	14,95	11,95	15,78	14,14	214	27	26	-162
Y4.12	29,97	15,00	11,78	15,33	14,64	214	25	25	-161

Table 5. Results of the test series 15x30 SE(B), a/W = 0.5, T = -120 °C.

Specimen	W [mm]	B [mm]	Bn [mm]	a0 [mm]	b0 [mm]	E [GPa]	KJc [MPa]	KJc(1T) [MPa]	T [°C]
A1.2	29,84	15,00	12,03	15,55	14,29	212	44	41	-120
A2.6	29,97	14,97	12,04	15,23	14,74	212	78	71	-121
Y1.6	29,98	14,93	12,00	15,50	14,48	212	82	74	-121
Y2.2	29,98	15,08	11,97	15,46	14,52	211	48	45	-120
Y2.12	29,95	14,98	12,03	15,38	14,57	212	61	56	-120
Y3.8	29,97	14,94	11,89	15,41	14,56	212	58	54	-121
Y4.4	29,98	15,04	12,00	15,58	14,40	212	40	38	-120
Y4.13	29,91	14,99	11,87	16,47	13,44	212	53	49	-120

Table 6. Results of the test series 15x30 SE(B), a/W = 0.5, T = -100 °C.

Specimer	W [mm]	B [mm]	Bn [mm]	a0 [mm]	b0 [mm]	E [GPa]	KJc [MPa]	KJc(1T) [MPa]	T [°C]
A1.4	29,97	14,96	12,02	15,46	14,51	210	121	109	-100
A3.2	29,91	15,03	12,07	15,51	14,40	210	83	75	-100
Y1.8	29,97	15,00	12,00	15,46	14,51	210	124	112	-101
Y2.13	29,92	14,96	12,03	15,51	14,41	210	106	95	-101
Y3.4	29,98	14,97	11,75	15,41	14,57	210	61	56	-101
Y3.10	29,97	14,97	12,00	15,40	14,57	210	104	93	-100
Y4.2	29,98	15,02	11,96	15,56	14,42	210	37	35	-100
Y4.6	29,97	15,02	12,80	15,50	14,47	212	77	70	-121

Table 7. Results of the test series 15x30 SE(B), a/W = 0.5, T = -85 °C.

Specimen	W [mm]	B [mm]	a0 [mm]	KJc [Mpa]	KJc (1T) [Mpa]	T [°C]
Y1.10	29.97	14.98	15.22	132	118	-85.0
Y1.4	29.99	14.99	15.15	100	91	-85.0
Y2.8	29.98	14.99	15.20	71	65	-85.0
Y3.12	29.97	14.97	15.12	87	79	-85.0
Y4.10	29.98	14.99	15.15	99	90	-85.0
A1.6	30.01	14.98	15.11	63	58	-85.0
A2.2	29.95	14.94	15.15	81	74	-85.0
A4.4	30.00	14.92	15.25	80	73	-85.0

Table 8. Results of the test series 15x30 SE(B), a/W = 0.5, T = -70 °C.

Specimen	W [mm]	B [mm]	a0 [mm]	KJc [Mpa]	KJc (1T) [Mpa]	T [°C]
Y1.12	29.97	15.01	15.22	126	113	-70.0
Y2.4	29.97	14.94	15.26	119	107	-70.0
Y3.2	30.00	14.91	15.21	91	82	-70.0
Y3.6	29.97	14.99	15.19	82	74	-70.0
Y4.8	29.97	15.02	15.20	102	92	-70.0
A2.4	29.99	14.94	15.23	111	100	-70.0
A3.6	29.98	15.03	15.23	102	92	-70.0
A4.2	29.96	14.95	15.19	63	58	-70.0

Table 9. Results of the test series 15x30 SE(B), a/W = 0.1, T = -160 °C.

Specimen	W [mm]	B [mm]	Bn [mm]	a0 [mm]	b0 [mm]	E [GPa]	KJc [MPa]	KJc(1T) [MPa]	T [°C]
Y1.3	29,96	15,00	11,95	3,45	26,51	214	45	42	-161
A1.1	29,82	15,00	12,00	4,13	25,69	214	60	55	-160
Y3.5	29,98	14,97	11,80	3,58	26,40	214	42	39	-161
Y2.1	29,80	14,97	11,80	3,51	26,29	214	30	29	-161
Y2.11	30,00	14,97	11,80	3,52	26,48	214	56	52	-161
A2.3	30,00	14,98	11,99	3,65	26,35	214	35	33	-161
Y4.7	29,98	15,01	11,94	3,62	26,36	214	27	26	-161
Y1.9	29,97	14,97	11,99	3,59	26,39	214	46	42	-153

Table 10. Results of the test series 15x30 SE(B), a/W = 0.1, T = -120 °C.

Specimen	W [mm]	B [mm]	Bn [mm]	a0 [mm]	b0 [mm]	E [GPa]	KJc [MPa]	KJc(1T) [MPa]	T [°C]
A1.3	29,99	15,00	11,70	3,62	26,37	212	48	45	-121
Y4.11	29,97	15,00	11,85	3,49	26,48	212	101	91	-120
Y1.5	29,97	14,99	11,85	3,45	26,52	212	141	126	-121
A3.5	29,97	14,97	11,80	3,45	26,52	212	90	81	-120
A4.7	29,97	14,96	11,85	3,42	26,55	212	76	69	-121
Y3.1	29,81	14,97	11,85	3,69	26,12	212	55	50	-121
Y4.9	29,97	14,99	11,85	3,55	26,42	212	56	52	-121
A3.1	29,80	14,97	11,85	3,87	25,93	212	75	68	-120

Table 11. Results of the test series 15x30 SE(B), a/W = 0.1, T = -100 °C.

Specimen	W [mm]	B [mm]	Bn [mm]	a0 [mm]	b0 [mm]	E [GPa]	KJc [MPa]	KJc(1T) [MPa]	T [°C]
A2.5	29,98	14,96	12,00	3,23	26,75	210	126	113	-100
A3.7	29,98	14,97	12,03	3,53	26,45	210	89	80	-100
A4.1	29,87	14,97	12,06	4,39	25,48	210	84	77	-100
Y1.1	29,85	14,95	11,90	4,05	25,80	210	106	96	-100
Y2.7	29,94	14,96	12,04	3,70	26,24	210	127	114	-100
Y3.3	29,95	14,98	11,95	3,44	26,51	210	110	99	-100
Y3.9	29,95	14,95	11,97	3,54	26,41	210	60	55	-101
Y4.5	29,97	15,00	12,04	3,83	26,14	210	100	90	-101

Table 12. Results of the test series 15x30 SE(B), a/W = 0.1, T = -85 °C.

Specimen	W [mm]	B [mm]	Bn [mm]	a0 [mm]	b0 [mm]	E [GPa]	KJc [MPa]	KJc(1T) [MPa]	T [°C]
Y3.7	29,97	15,13	12,11	3,62	26,35	209	64	59	-85
Y4.3	30,00	15,01	11,89	3,72	26,28	209	107	96	-85
Y2.5	29,99	14,97	11,96	3,48	26,51	209	172	153	-86
A1.5	29,96	15,04	12,03	3,60	26,36	209	78	71	-85
A4.3	30,00	14,94	11,90	3,70	26,30	209	62	56	-85
A2.7	29,99	15,04	11,94	3,60	26,39	209	91	82	-85
Y1.11	29,95	15,02	11,92	3,81	26,14	209	373	330	-85
A2.1	30,06	14,97	11,89	3,96	26,10	209	117	105	-85

Table 13. Results of the test series 15x30 SE(B), a/W = 0.1, T = -70 °C.

Specimen	W [mm]	B [mm]	a0 [mm]	KJc [Mpa]	KJc (1T) [Mpa]	T [°C]
A1.7	30.02	14.86	3.10	239	211	-70.0
A3.3	29.99	14.97	3.14	115	103	-70.0
A4.5	29.99	14.88	3.17	146	131	-70.0
Y1.7	29.96	14.83	3.21	298	263	-70.0
Y2.3	29.96	14.94	3.16	209	185	-70.0
Y2.9	29.96	14.92	3.07	129	116	-70.0
Y3.11	29.97	14.97	3.18	108	97	-70.0
Y4.1	29.80	14.95	2.91	77	70	-70.0

6 DISCUSSION

Figure 16 shows the fracture toughness results obtained with the 5x10 and 15x30 SE(B) specimens. The T_0 obtained with 5x10 SE(B) specimens is -86 °C, σ = 7 °C, and T_0 is -79 °C, σ = 5.7 °C, obtained with 15x30 SE(B) specimens. The uncertainty in the results is larger than the difference between the obtained T_0 estimates, thus, indicating no significant difference between the T_0 obtained with 15x30 SE(B) and 5x10 SE(B) specimens. However, the specimen extraction location in thickness direction influences the obtained fracture toughness. Figure 17 compares the results obtained with shallow cracked specimens (a/W = 0.1) and specimens with deep cracks (a/W = 0.5).

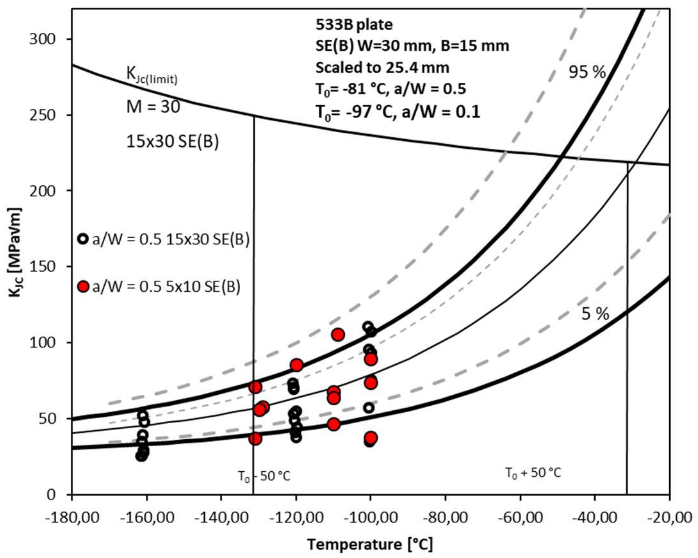

Figure 16. Comparison between 5x10 and 15x30 SE(B) specimens. T0 = -81 °C is calculated for both the 5x10 and 15x30 SE(B) specimens with a/W = 0.5.

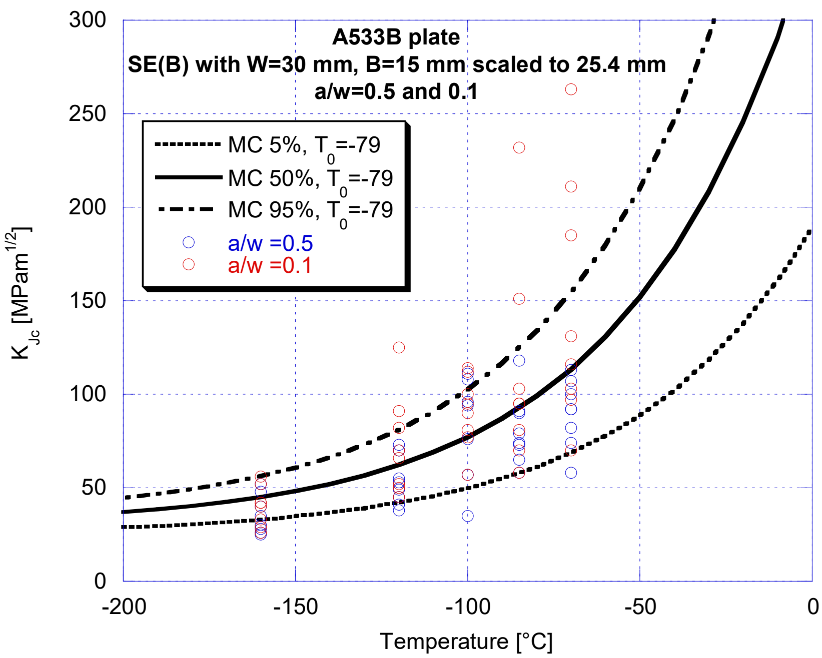

Figure 17. Comparison between specimens with shallow and deep cracks.

The effect of specimens extraction location on fracture toughness is analysed in the figures 18 and 19. The data in figure 18 was normalized by estimating the failure probability according to the Master Curve and estimating the corresponding fracture toughness at -100 °C. The results indicate that the fracture toughness is higher closer to the surface than at the center of the plate. The effect is less apparent on the other side of the plate, possibly due to smaller amount of observations. Figure 19 shows that the fracture toughness may also be affected by the extraction location in the transverse width direction of the plate. The high failure probability is connected to high fracture toughness.

Therefore, the difference in T_0 between 5x10 and 15x30 SE(B) specimens is affected by the specimen extraction location, the 15x30 SE(B) specimens were also extracted close to the center where the fracture toughness is lower, thus, increasing the T_0. Figure 18 indicates that the 5x10 SE(B) specimens can yield higher fracture toughness. This can occur if the smaller sampling volume of a 5x10 SE(B) specimen does not capture the weakest microstructural features. However, this needs to be confirmed through microstructural investigations in future studies.

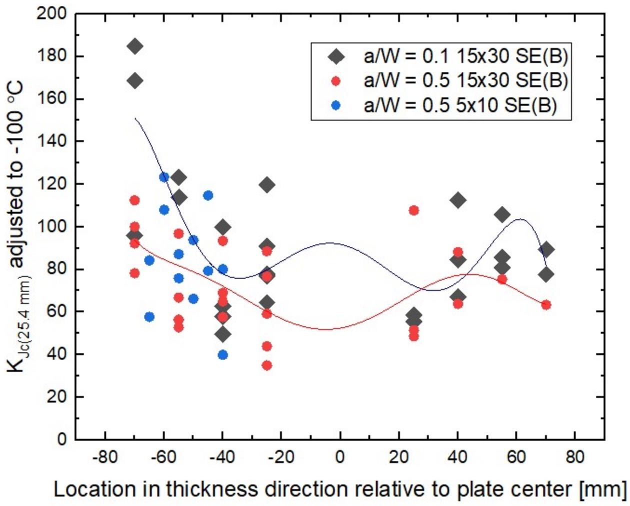

Figure 18. Variation in fracture toughness in the thickness direction. The fracture toughness data has been normalized.

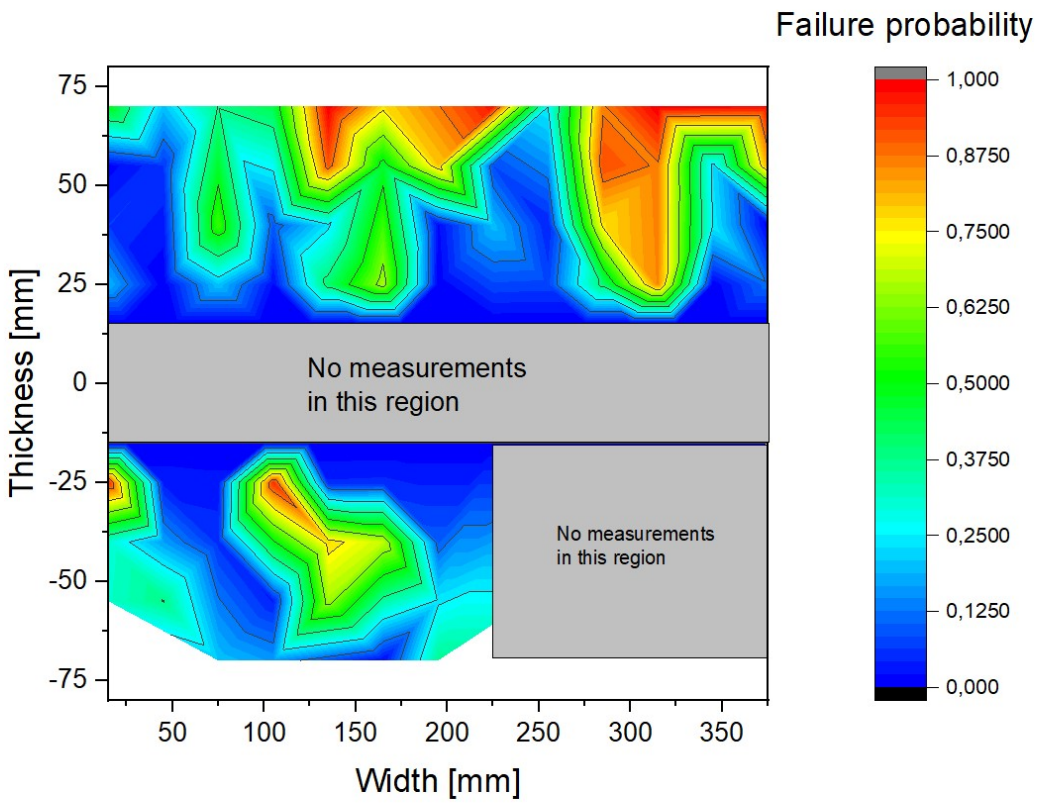

Figure 19. The fracture toughness is higher in the red areas and lower in the blue areas.

Another part of the same JRQ ASTM A533 grade B class 1 plate has previously been characterised in [1]. Figure 20 shows the T_0 in the thickness direction of the plate. Fracture toughness is higher at the surface than at the center of the plate. Figure 21 shows the fracture toughness results from [1] and describes the material properties at ¼ thickness. The orientation of the specimens is T-L, thus, deviating from the orientation of the specimens characterized in this study. The T_0 is slightly higher for the T-L orientation, -72 °C. The multimodal inhomogeneity analysis was performed on the data, indicating that the data is moderately inhomogeneous, $T_{0,MML}$ = -72 °C (maximum likelihood concept, MML) and σ_{MML} = 11 °C. The same values for the fracture toughness results from this study are $T_{0,MML}$ = -73 °C and σ_{MML} = 18 °C. The slightly larger σ_{MML} can be caused by extraction of the specimens from a wider range than only the ¼ thickness.

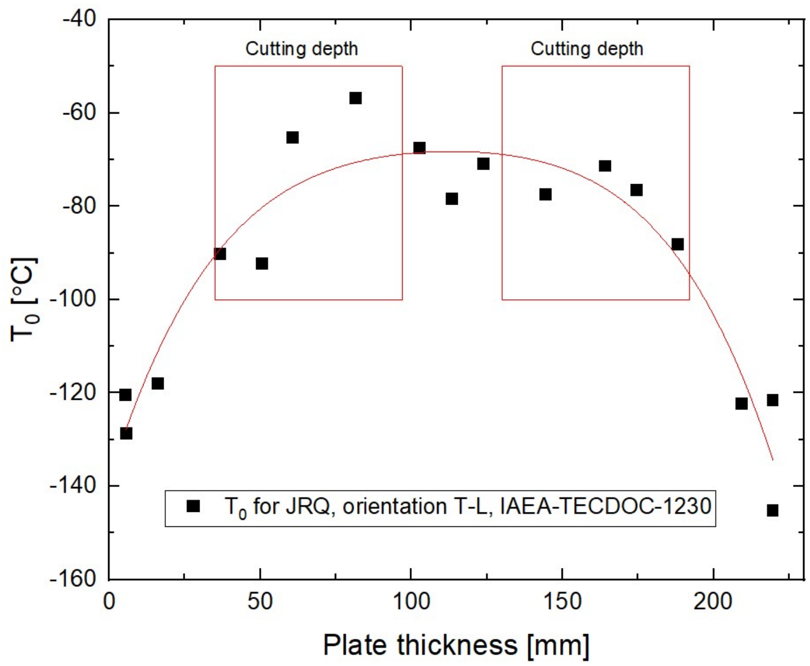

Figure 20. Variation in T0 in thickness direction for JRQ plate from [1]. Specimen orientation T-L.

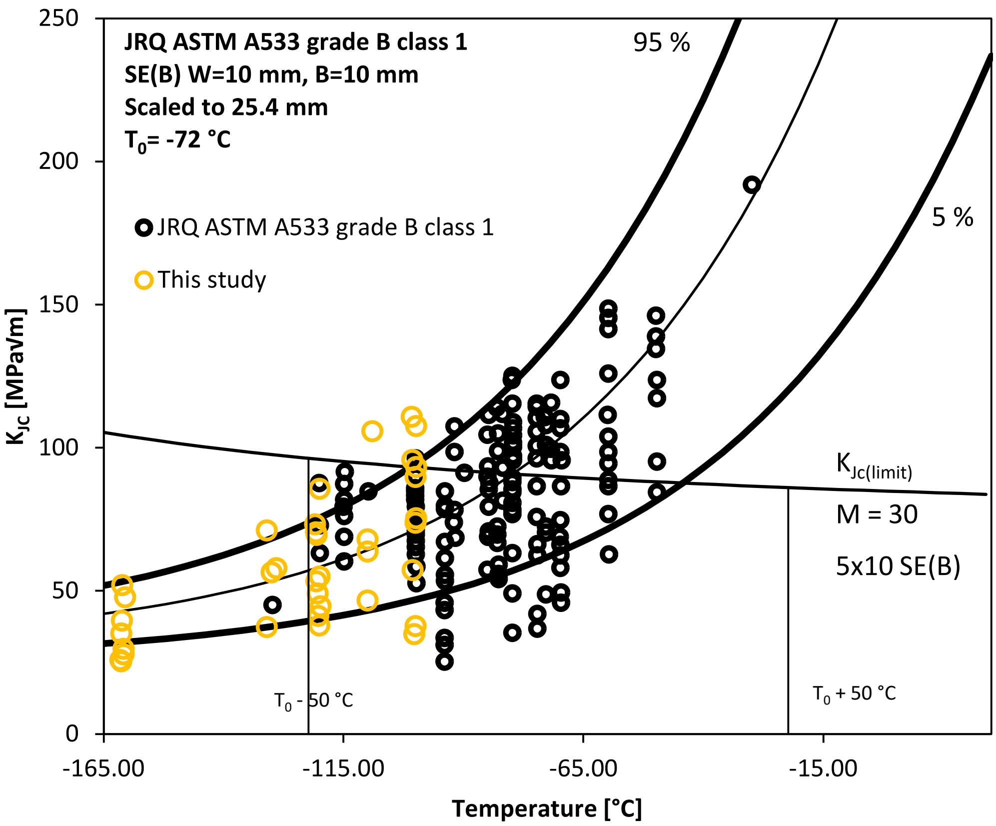

Figure 21. Comparison between the fracture toughness results from this study and the results from [1]. The orientation is T-L in [1] and the results are from 1/4T. The Master Curve is fitted to the data from [1].

7 CONCLUSION

The objective of the work conducted in 2020 was to produce data for fracture mechanical analysis, and scientific articles done in the upcoming years in the NKS project WPS-MAF. The results show that that the T_0 obtained with 15x30 SE(B) specimens is in the same range as the T_0 obtained with 5x10 SE(B) specimens. The fracture toughness of the ASTM A533 grade B class 1 plate, 230 mm thick, is higher closer to the surface than at the center, which agrees with previous investigations. Further metallography and post processing work will be done to the 5x10 SE(B) specimens to analyse the differences to the 15x30 SE(B) specimens. The results are applied also for analyses of the effect of crack front curvature on fracture toughness.

8 ACKNOWLEDGEMENT

The authors are grateful for the financial support from NKS and SAFIR.

9 DISCLAIMER

10 REFERENCES

[1] Brumovsky M, Davies LM, Kryukov A, Kyssakov VN, Nanstad RK. Reference manual on the IAEA JRQ correlation monitor steel for irradiation damage studies. IAEA-TECDOC-1230. Nucl Power Eng Sect IAEA 2001.

Bibliographic Data Sheet **NKS-446**

Title	WPS-MAF, Report on design and results from experimental test program for material characterization
Author(s)	Tobias Bolinder[1], Alexander Eriksson[1] Jonas Faleskog[2], Magnus Boåsen[2] Sebastian Lindqvist[3], Veera Peltonen[3]
Affiliation(s)	[1]Kiwa Inspecta Technology AB, Stockholm, Sweden [2]Royal Institute of Technology, Department of Solid Mechanics, Stockholm, Sweden [3]VTT, Helsinki, Finland
ISBN	978-87-7893-538-0
Date	April 2021
Project	NKS-R / WPS-MAF
No. of pages	20
No. of tables	13
No. of illustrations	21
No. of references	1
Abstract max. 2000 characters	In this report, the VTT and KTH experimental results are presented. The characterization of the ductile to brittle transition region was done with small 5x10 single-edge bend specimens (SE(B)) and 15x30 SE(B) specimens in different temperatures. The characterization with 15x30 SE(B) specimens were done with deep and shallow cracks. The characterization was completed by metallography characterization of the 533B plate. This is an interim report related to the characterization and development work done in WPS-MAF. The results are utilized later in the project.
Key words	Warm pre-stressing, Cleavage fracture, Failure probability, Fracture toughness, Fracture experiments, Non-local probabilistic model, Master Curve

Available on request from the NKS Secretariat, P.O.Box 49, DK-4000 Roskilde, Denmark.
Phone (+45) 4677 4041, e-mail nks@nks.org, www.nks.org